*Research Article* *Volume 5, Issue 3*

JCMCRI

Journal of Clinical & Medical Case Reports, Images

Received: March 09, 2026 Published: March 19, 2026

DOI: 10.55920/3064-8025/1177

# Pilot Experimental Study of Different Types of Vascular Grafts Remodeling in the Posterior Vena Cava System of Growing Primates

**AA Zakharenko[1]*, GI Popov[1], NN Gurgenidze[1], AA Suprunovich[1], MA Kondrashov[1], AV Belozertseva[1], NA Zavrazhnykh[3,4], G Yukina[1], EG Sukhorukova[1], IA Paltyshev[1], AA Kutenkov[1], DA Zaitsev[5], AA Trushin[1], AN Gracheva[2], VE Yudin[3,4], GG Khubulava[1], SV Orlov[1,6] and SF Bagnenko[1]**

*[1]IP Pavlov First St. Petersburg State Medical University, St. Petersburg, Russia*

*[2]IM Sechenov First Moscow State Medical University (Sechenov University), Moscow, Russia*

*[3]BP Konstantinov Petersburg Nuclear Physics Institute, National Research Center "Kurchatov Institute" - Institute of Macromolecular Compounds, St. Petersburg, Russia*

*[4]Peter the Great St. Petersburg Polytechnic University, St. Petersburg, Russia*

*[5]NN Petrov National Medical Research Center of Oncology, St. Petersburg, Russia*

*[6]Kurchatov Complex of Medical Primatology - National Research Center "Kurchatov Institute", Sochi, Russia*

## Abstract

**Objective:** To perform a comparative analysis of remodeling processes in various types of vascular implants under conditions of ongoing physiological growth using an experimental primate model.

**Materials and methods:** A pilot prospective experimental study with a parallel design was conducted from June 2022 to November 2024 at the Kurchatov Complex of Medical Primatology (Sochi) and Academician I.P. Pavlov First St. Petersburg State Medical University. The study involved 6 male hamadryas baboons (Papio hamadryas) that underwent resection of the infrarenal segment of the posterior vena cava followed by prosthetic replacement. Five graft types were evaluated: polytetrafluoroethylene (PTFE) prosthesis, a biodegradable polymer matrix based on poly(L-lactide) and poly(ε-caprolactone), single-group and cross-group allografts, and autologous vein. The follow-up period was 29 months. Comprehensive assessment included direct intraoperative morphometry, duplex ultrasound scanning (DUS) with hemodynamic parameter analysis, spiral computed tomographic angiography (SCTA), and histopathological examination.

**Results:** The adequacy of the experimental model was confirmed by significant increases in growth and weight parameters in all animals. The autologous vein demonstrated balanced dilatational remodeling: length increased by 20%, diameter by 40–50%, with complete integration and stable hemodynamics. Allogeneic implants (both single-group and cross-group) exhibited significant but variable adaptive potential: length gain reached 58–67%, functional status was satisfactory, but diameter changes were multidirectional, justifying the need for dynamic DUS monitoring. The biodegradable matrix showed maximal length increase (+42%) with transient constrictive remodeling: lumen narrowing by 33% in the early period followed by diameter restoration by the end of the experiment; intimal hyperplasia was absent, and hemodynamic parameters stabilized. The PTFE prosthesis thrombosed and showed no signs of adaptation.

**Conclusion:** The autologous vein remains the "gold standard." Allogeneic grafts represent a clinically acceptable alternative but require regular monitoring. The biodegradable matrix, exhibiting growth potential and reversible constriction, is considered a promising material for further optimization. The combination of morphometry and DUS represents an optimal methodological approach for preclinical evaluation of vascular implants intended for a growing organism.

**Keywords:** Vascular prosthesis, allograft, autologous vein, biodegradable scaffold, remodeling, growing organism, experimental model, primates, ultrasound monitoring, posterior vena cava.

## Introduction

Reconstruction of major veins in children, particularly in oncological diseases requiring venous resection, remains one of the most challenging problems in pediatric surgery [1]. The main factor determining long-term outcomes of such interventions is the ongoing somatic growth of the patient, which imposes specific requirements on the biological and synthetic materials used for grafting [2,3]. Traditionally applied methods, including synthetic polytetrafluoroethylene (PTFE) prostheses, as well as auto- and allografts, have several limitations in pediatric practice. The most significant among these are the high risk of thrombosis, lack of growth potential, progressive calcification, and degenerative changes in the vascular wall, which can ultimately lead to restenosis, occlusion, and the need for repeated surgical interventions [4,5].

In this context, developments in the field of tissue engineering aimed at creating a new generation of biodegradable vascular grafts are of particular relevance. Such constructs are potentially capable of active remodeling, integration into recipient tissues, and, most importantly, adaptive growth in parallel with the developing organism [6,7]. Current preclinical research encompasses a wide range of materials, from modified synthetic polymers to fully resorbable extracellular matrices colonized with autologous cells [8]. A key condition for the successful functioning of such implants is their rapid and complete

***Corresponding Author:** *AA Zakharenko, IP Pavlov First St. Petersburg State Medical University, St. Petersburg, Russia

**Citation: AA Zakharenko*, Pilot Experimental Study of Different Types of Vascular Grafts Remodeling in the Posterior Vena Cava System of Growing Primates.** Jour of Clin & Med Case Rep, Imag 2026; 5(3): 1177.

endothelialization, ensuring long-term patency, stable hemodynamic parameters, and biocompatibility [9].

The transition from experimental laboratory developments to clinical application is impossible without thorough preclinical evaluation on adequate biological models [10]. The choice of experimental model plays a decisive role in predicting outcomes in humans. Large mammals, and especially primates, due to the anatomical and physiological similarity of the cardiovascular system, hemodynamic parameters, and immune responses, are considered the most relevant platform for studying the biocompatibility, remodeling processes, and long-term functioning of vascular implants [11,12]. However, the number of studies devoted to the direct comparative analysis of the behavior of different graft classes (synthetic, allogeneic, and tissue-engineered) specifically under conditions of active growth, modeling the pediatric population, remains limited.

Considering the above, this pilot study was initiated to develop and validate an experimental model in growing primates for a comprehensive comparative assessment of remodeling processes in different types of vascular implants during major vein replacement.

**Objective:** To determine the optimal type of vascular graft characterized by the best adaptation and integration under conditions of ongoing recipient growth.

**Research tasks:**
Perform a chronic experiment on replacement of the infrarenal segment of the posterior vena cava in growing primates using five types of grafts: PTFE prosthesis, biodegradable polymer matrix, single-group and cross-group allografts, and autologous vein.

Conduct a dynamic assessment of somatic growth of the animals, functional state of the implants, and their hemodynamic characteristics (linear and volumetric blood flow velocities, pressure gradient) during a long-term postoperative period.

Perform macroscopic, morphometric, and histopathological examination of explanted samples upon completion of the experiment.

Based on a comprehensive analysis of the obtained data, determine the most effective graft type in terms of its ability for structural and functional remodeling under conditions of active body growth.

## Materials and Methods

**Study design and ethical approval:** A pilot prospective experimental study with parallel comparison groups was conducted from June 2022 to November 2024 at the Kurchatov Complex of Medical Primatology (Sochi) and Academician I.P. Pavlov First St. Petersburg State Medical University. The study protocol was approved by the Local Ethics Committee of the Kurchatov Complex (Protocol No. 02-9 pr dated November 19, 2024). The study was performed in accordance with the principles of the Declaration of Helsinki, European Directive 2010/63/EU, and the Russian Ministry of Health Order No. 199n dated April 1, 2016 "On Approval of the Rules of Good Laboratory Practice".

**Animals and housing conditions:** Six clinically healthy male hamadryas baboons (Papio hamadryas) aged 15–20 months (mean age 17.67 ± 2.42 months) with a body weight of 4850 ± 920 g were included in the experiment. The animals were obtained from a certified breeding colony. Inclusion criteria were age corresponding to the active phase of somatic growth, absence of chronic diseases, and normal hematological and biochemical blood parameters. All animals were housed under standard vivarium conditions with controlled microclimate, a 12/12 h light/dark cycle, and free access to water and a standard primate diet.

**Vascular grafts:** Five types of grafts were used (Table 1). The synthetic prosthesis was made of expanded polytetrafluoroethylene (PTFE, Ecoflon, Russia) with a diameter of 6 mm. The biodegradable polymer matrix (BPM) was a tubular scaffold with an inner layer of poly(L-lactide) and an outer layer of poly(ε-caprolactone) fabricated by electrospinning; its diameter was 4 mm and wall thickness 250 µm. Allogeneic grafts (single-group and cross-group) were harvested from donor baboons participating in the study. After removal, the vein segment was placed in Custodiol solution for initial preservation, then decontaminated in RPMI-1640 medium with L-glutamine supplemented with antibiotics and antimycotics (vancomycin 500 mg/L, ciprofloxacin 150 mg/L, metronidazole 200 mg/L, fluconazole 50 mg/L) at +4°C for 24 h. After rinsing with sterile saline, the grafts were stored in fresh RPMI-1640 medium at +4°C until implantation. The autologous vein (autovein) was the infrarenal segment of the posterior vena cava harvested from the same animal immediately prior to grafting.

***Table 1:*** Characteristics of experimental animal groups.

| Animal | Intervention | Material | Number (n) |
|---|---|---|---|
| No. 1 | Posterior vena cava (PVC) resection with grafting | PTFE prosthesis | 1 |
| No. 2 | PVC resection with grafting | Biodegradable polymer matrix | 1 |
| No. 3 | PVC resection with allografting | Single-group allograft | 1 |
| No.4, 6 | PVC resection with autografting | Native autologous vein | 2 |
| No. 5 | PVC resection with allografting | Cross-group allograft | 1 |

**Surgical procedure:** After a 12-h fasting period, animals underwent premedication, induction, and maintenance of anesthesia. A midline laparotomy was performed. The infrarenal segment of the posterior vena cava (mean length 43 ± 5.1 mm) was mobilized and resected. Reconstruction was carried out by interposition of the corresponding graft. End-to-end vascular anastomoses were created under an operating microscope (Carl Zeiss OPMI Pico) using interrupted 9-0 polypropylene sutures (Prolene, Ethicon). The mean operation time was 179 ± 16.43 min. Intraoperative blood loss did not exceed 5 mL.
**Postoperative management:** It included analgesia, antibiotic prophylaxis with ceftriaxone (50 mg/kg/day for 5 days), anticoagulant therapy with enoxaparin (1.5 mg/kg/day subcutaneously for 3 days), and continuous oral administration of acetylsalicylic acid (10 mg/day).

**Follow-up protocol:** The total observation period was 29 months. Monthly clinical examinations, morphometry (body weight, body length), and duplex ultrasound scanning (DUS) using a Vivid E95 device (General Electric, USA) were performed. DUS assessed graft morphometric parameters (length, lumen diameter, wall thickness) and hemodynamic indices: peak systolic velocity (PSV), end-diastolic velocity (EDV), time-averaged maximum velocity (TAMax), time-averaged mean velocity (TAmean), and pressure gradient (PG). At months 4, 12, and 29, spiral computed tomographic angiography (SCTA) with bolus contrast enhancement was performed to evaluate patency and morphometry (Figure 1).

**Figure 1:** *Experimental stages:* **(a)** *endotracheal anesthesia administration;* **(b)** *surgical implantation of the vascular graft;* **(c)** *implant monitoring by duplex ultrasound scanning (DUS) and animal morphometry;* **(d)** *spiral computed tomographic angiography (SCTA) performance.*


**Histopathological analysis:** The experiment was terminated by a second surgical intervention with explantation of the grafts and ligation of the posterior vena cava immediately below the renal vessels. Specimens were fixed in 10% neutral buffered formalin, routinely processed, and embedded in paraffin. Sections of 4–5 µm thickness were stained with hematoxylin and eosin and Mallory's trichrome. Cellular infiltration, wall structure, presence of thrombi, calcification, and neointimal status were evaluated.

**Statistical analysis:** Data are presented as mean ± standard deviation (M ± SD). Paired Student's t-test or Wilcoxon signed-rank test was used for comparisons depending on data distribution. Differences were considered statistically significant at $p < 0.05$. Analysis was performed using IBM SPSS Statistics 26.0.

## Results

**Study attrition:** Animal No. 4 died at 28 months of follow-up from progressive chronic kidney disease associated with urolithiasis, which was unrelated to vascular graft function.

**Somatic growth dynamics:** During the 29-month observation period, significant growth of all experimental animals was recorded, confirming the adequacy of the chosen model of a growing organism. Mean body weight increased by 36.15% from 4850±840 g to 6603±898 g ($p<0.01$). Mean body length increment was 64.83 mm ($p<0.01$).

Analysis of individual linear growth trajectories revealed pronounced positive dynamics in all animals (Figure 2a). The rate of body length increase, assessed by linear regression, varied between individuals, reflecting natural biological variability. High coefficients of determination ($R^2$), reaching 87.5% and 73.5% in animals No. 3 and No. 4, respectively, indicated stable and predictable somatic growth throughout the observation period.

**Figure 2a:** *Individual dynamics of body length in animals over 29 months of observation. The y-axis represents body length as a percentage of baseline; the x-axis represents time in months. Solid lines indicate individual linear regressions for each animal (n=6). The dashed line represents the overall trend (group mean).*

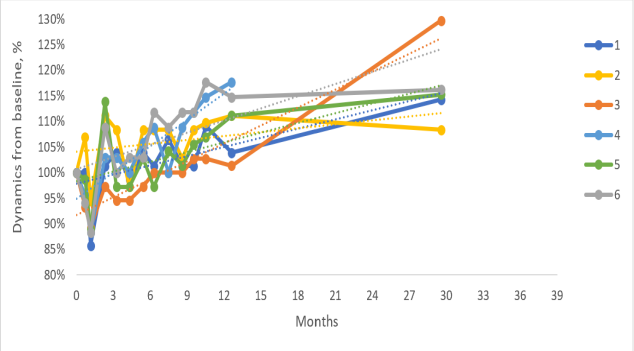


Body weight dynamics also showed a consistent positive trend with significant interindividual variability (Figure 2b). Monthly weight gain rates ranged from 0.63% to 5.41%. The highest average monthly weight gain rate (5.41%/month) was observed in animal No. 4. Animals No. 3 and No. 4 exhibited high coefficients of determination ($R^2>0.90$), confirming the linear and predictable nature of body weight gain. Thus, the documented positive dynamics of two key somatometric parameters-body length and body weight-confirm that the entire experimental period occurred during an active phase of somatic growth, a fundamental condition for valid assessment of vascular implant remodeling in a setting modeling the growing pediatric organism.

***Figure 2b:*** *Individual dynamics of body weight in animals over 29 months of observation. The y-axis represents body weight as a percentage of baseline; the x-axis represents time in months. Solid lines indicate linear regression lines for each animal (n=6). The dashed line represents the group mean trend.*

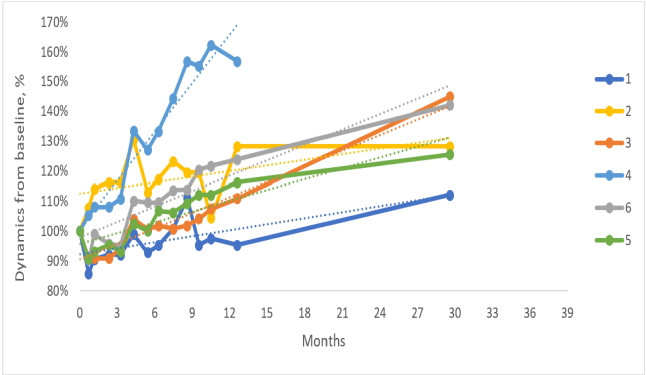


**Summary analysis of vascular graft remodeling:** To comparatively evaluate remodeling of different vascular implant types, key morphometric and hemodynamic parameters were analyzed. Figure 3 presents the results of direct intraoperative measurements of graft length and diameter at implantation and after explantation. Figure 4 reflects the long-term dynamics of these same parameters according to duplex ultrasound scanning (DUS). Figure 5 shows the dynamics of volumetric blood flow velocity, characterizing the hemodynamic load on the implants.

***Figure 3a:*** Length of vascular grafts at the time of implantation and after explantation according to direct intraoperative morphometry (mm).

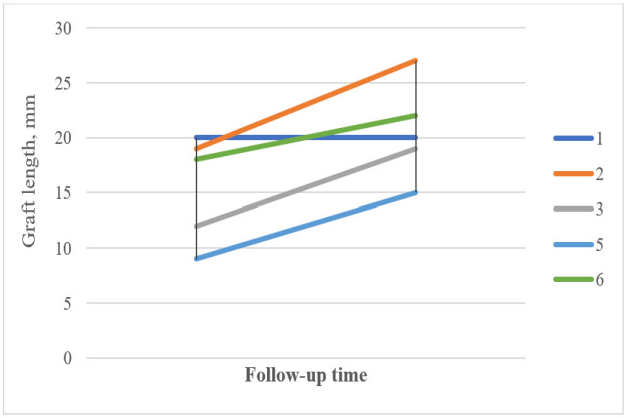


***Figure 3b:*** Lumen diameter of vascular grafts at the time of implantation and after explantation according to direct intraoperative morphometry (mm).

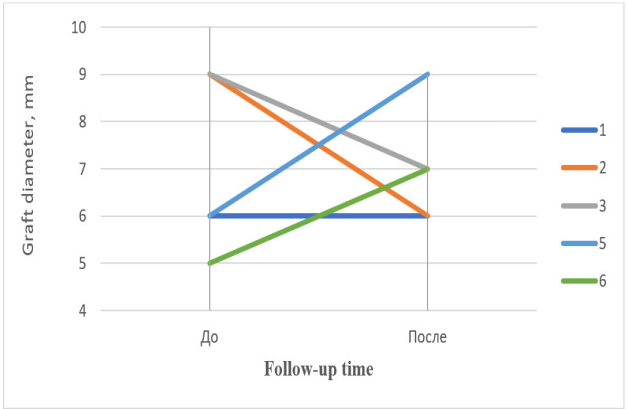


***Figure 4a:*** Dynamics of absolute length of vascular grafts according to duplex ultrasound scanning (DUS) over 12 months of follow-up. Solid lines represent linear regression for each animal. The dashed line represents the overall trend.

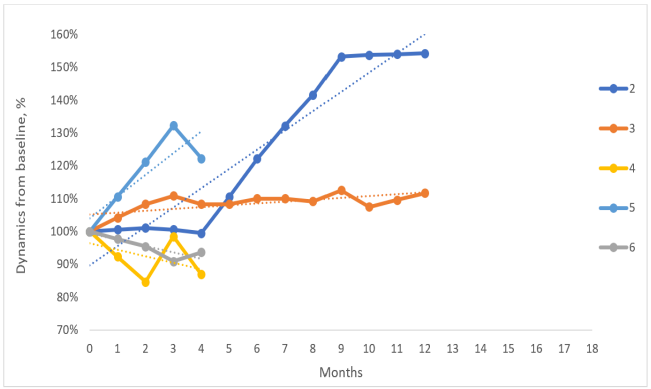


***Figure 4b:*** Dynamics of functional lumen diameter of vascular grafts according to duplex ultrasound scanning (DUS) over 10 months of follow-up. Solid lines represent linear regression for each animal. The dashed line represents the overall trend.

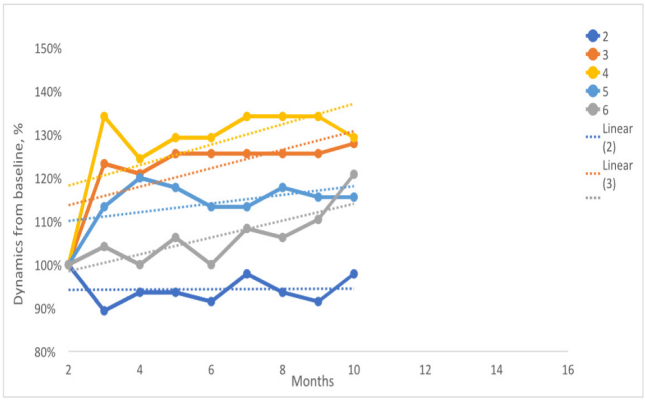


***Figure 5:*** Dynamics of volumetric blood flow velocity through vascular grafts over 11 months of follow-up. Changes are shown as a percentage of the baseline postoperative level (n=5). Solid lines represent individual trajectories; the dashed line represents the group trend (linear regression of mean values).

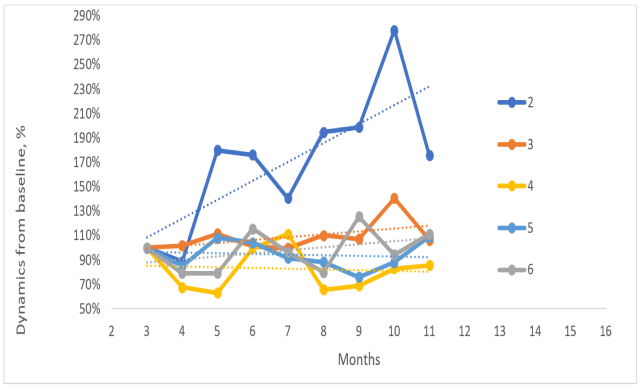


**Autologous vein:** The autologous vein graft demonstrated an exemplary balanced type of remodeling. Direct morphometry (Figure 3 a, b) showed a mean graft length increase of 20% (from 15.5 to 18.5 mm) and a diameter increase of 40–50%. Dynamic DUS confirmed a stable dilatational trend: functional diameter increased by 25–30% by the end of observation, and positive length dynamics were also recorded (Figure 4 a, b). Hemodynamic parameters remained stable, and the increase in volumetric blood flow velocity was minimal (Figure 5). Follow-up SCTA clearly demonstrated preserved patency in the autologous vein implantation zone (Figure 6 a, b). At explantation, the autologous vein macroscopically did not differ from the native vein (Figure 7 a, b). Histopathological examination revealed preservation of a three-layer wall structure close to native; inflammatory

reaction was absent in all layers, except for minimal inflammatory infiltration in the anastomosis zone; no signs of intimal hyperplasia were detected (Fig. 8 a, b). These data morphologically substantiate the successful integration and functional integrity of the autologous vein.

***Figure 6:*** SCTA follow-up of the autologous vein implanted into the infrarenal segment of the posterior vena cava in animal No. 6: (a) follow-up at 12 months; (b) follow-up at 29 months.

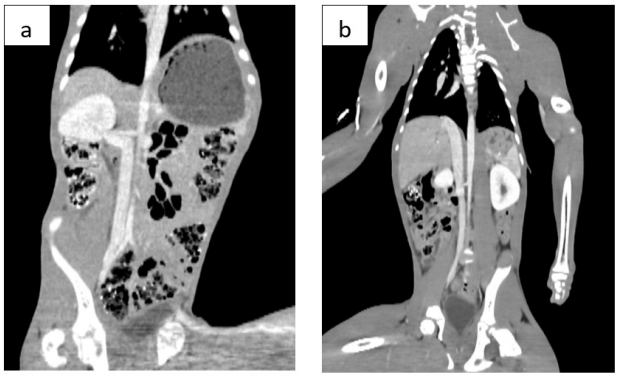


***Figure 7:*** Macroscopic appearance of the autologous vein in animal No. 6.
(a) Intraoperative image during primary implantation.
(b) Appearance of the graft 29 months after implantation. Complete macroscopic similarity to the native vein is noted, with no evidence of significant cicatricial-adhesive process or tissue infiltration.

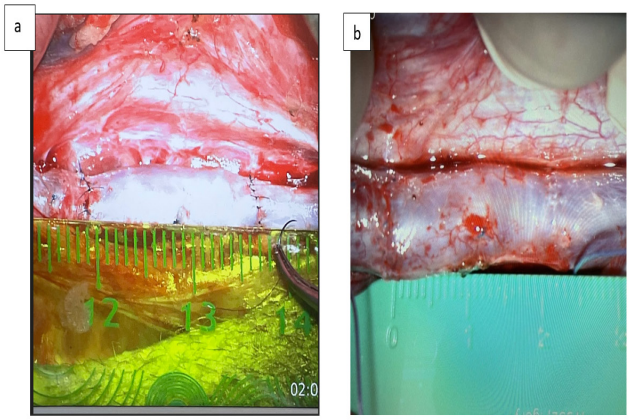


***Figure 8:*** Autologous vein implant 29 months after implantation: (a) panoramic view; (b) fragment of the implant wall at higher magnification. Hematoxylin and eosin staining, magnification ×4 (a), ×10 (b). Designations: 1 - intima, 2 - media, 3 - adventitia. The wall structure is preserved; no signs of inflammation or intimal hyperplasia are present.

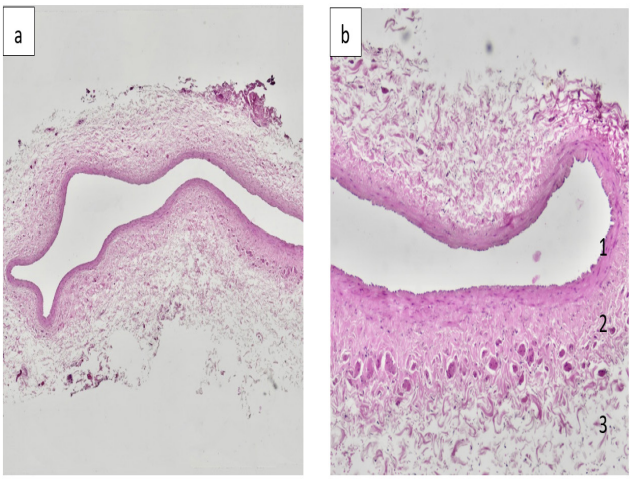


**Allogeneic grafts:** Allogeneic implants exhibited significant but variable adaptive potential.

*Single-group allograft.* Direct morphometry recorded a substantial length increase (+58%, from 12 to 19 mm) with constrictive change in anatomical diameter (–22%, from 9 to 7 mm) (Figure 3 a, b). Conversely, dynamic DUS revealed an opposite trend- an increase in functional diameter by 16% during the observation period (Figure 4 a, b). This discrepancy highlights the difference between structural changes assessed ex vivo and functional status in vivo. Hemodynamic parameters remained stable (Figure 5). SCTA data confirmed preserved blood flow in the implantation zone (Figure 9a,b). Macroscopic examination of the explanted graft showed no differences from the native vein, no cicatricial deformation, and no signs of stenosis (Figure 10a,b). Histological analysis demonstrated preservation of a three-layer wall structure close to native, with minimal inflammatory reaction. In the anastomosis zone, a smooth transition of the native vein intima onto the allograft was observed, with no neointimal hyperplasia (Figure 11a,b). This explains the clinically acceptable integration of this graft type despite the variability in instrumental data.

*Cross-group allograft.*

***Figure 9:*** SCTA follow-up of the single-group allograft implanted into the infrarenal segment of the posterior vena cava (animal No. 3): (a) follow-up at 12 months; (b) follow-up at 29 months. Satisfactory patency of the reconstruction zone is preserved.

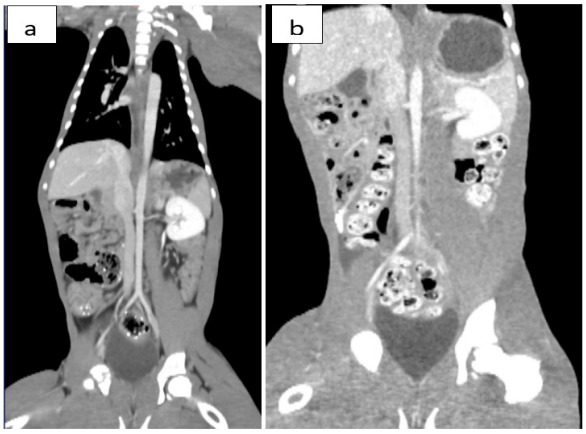


***Figure 10:*** Macroscopic appearance of the single-group allogeneic graft in animal No. 3.
(a) Intraoperative image during primary implantation.
(b) Appearance of the graft 29 months after implantation. The graft is macroscopically indistinguishable from the native vein, with no signs of cicatricial process, deformation, or stenosis.

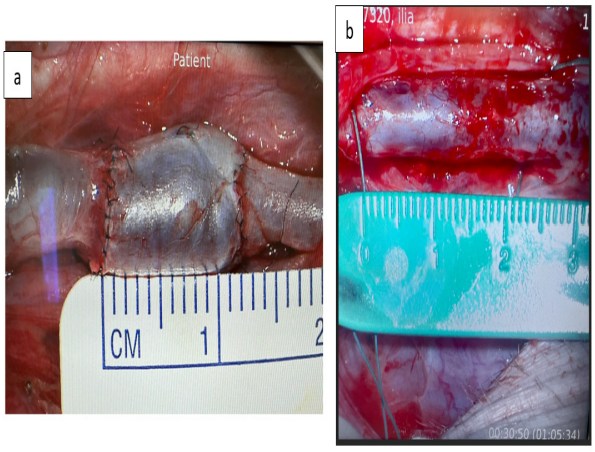

***Figure 11:*** *Single-group allogeneic implant 29 months after implantation:* **(a)** *panoramic view of the anastomotic zone;* **(b)** *fragment of the implant wall. Hematoxylin and eosin staining, magnification ×4 (a), ×10 (b). Designations: 1 - intima, 2 - media, 3 - adventitia. The black arrow indicates the smooth transition of the native vein intima onto the implant (anastomotic zone). The wall structure is preserved; no intimal hyperplasia is observed.*

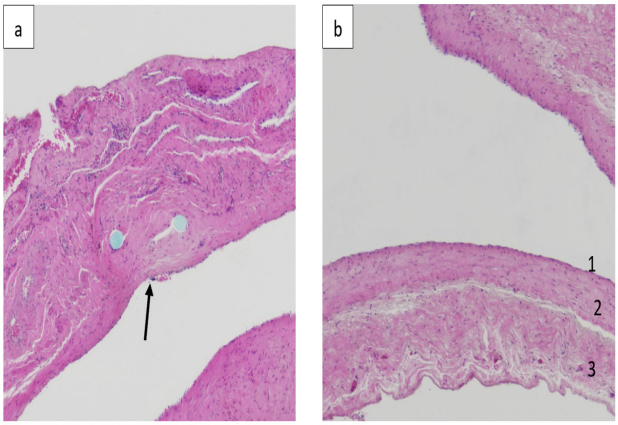


The maximum relative length increase (+67%, from 9 to 15 mm) and anatomical diameter increase of 50% (from 6 to 9 mm) were recorded by morphometry (Fig. 3 a, b). However, DUS showed that the functional lumen of the graft remained virtually unchanged (+0.2%) (Figure 4 a, b), likely related to the development of endothelial hyperplasia visualized as "small tubercles" (Figure 12 a). SCTA confirmed satisfactory contrast enhancement of the anastomosis zone (Figure 12 b, c). At explantation, macroscopic infiltration of perigraft tissues was noted (Figure 13 a, b). Histopathological examination revealed regression of smooth muscle cells in the media and their absence in the adventitia, indicating partial wall degradation due to immune response (Figure 14). Inflammatory reaction in the adventitia was minimal, and anastomotic zones showed a smooth transition of the native vein intima onto the implanted material without signs of hyperplasia.

***Figure 12:*** Cross-group allograft (animal No. 5): (a) ultrasound image demonstrating features characteristic of intimal/endothelial hyperplasia; (b) SCTA follow-up at 12 months after implantation; (c) SCTA follow-up at 29 months after implantation. Satisfactory patency of the reconstruction zone is preserved.

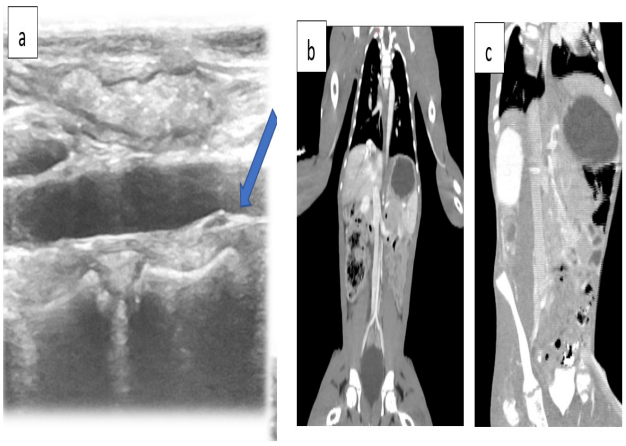


***Figure 13:*** Macroscopic appearance of the cross-group allogeneic graft in animal No. 5.
(a) Intraoperative image during primary implantation.
(b) Appearance of the graft 29 months after implantation. The graft is macroscopically indistinguishable from the native vein; however, signs of perigraft tissue infiltration with the formation of dense adhesions are visualized (indicated by the arrow).

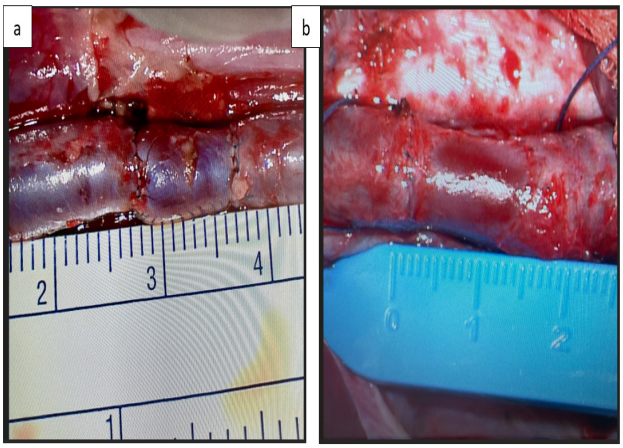


***Figure 14:*** *Fragment of the cross-group allogeneic implant wall 29 months after implantation. Hematoxylin and eosin staining, magnification ×10. Designations: 1 - intima, 2 - media, 3 - adventitia. Regression of smooth muscle cells in the media and their absence in the adventitia are observed.*

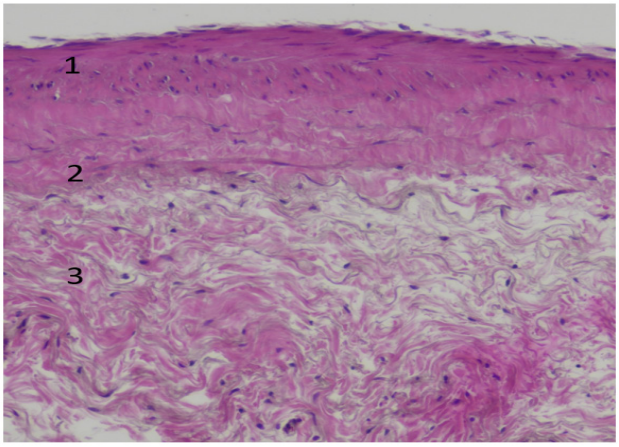


**Biodegradable polymer matrix (BPM):** BPM demonstrated a unique, phased remodeling pattern fundamentally different from the other studied graft types.

The largest absolute length increase among all implants was recorded: +42% (from 19 to 27 mm), confirmed by both direct intraoperative morphometry and dynamic DUS monitoring (Figure 3 a, 4 a). This indicates the high adaptive capacity of the matrix to conditions of ongoing somatic growth. In the early postoperative period, constrictive remodeling was noted: anatomical diameter decreased by 33% (Figure 3 b), and the functional lumen according to DUS narrowed by approximately 15% (Figure 4 b). However, by the end of the observation period, a consistent trend towards diameter restoration to near-baseline values was observed. The identified constriction was transient and reversible, not a progressive stenotic process.

Initial increases in linear velocity and decreases in volumetric blood flow velocity were subsequently normalized (Figure 5). By the end of observation, the pressure gradient had stabilized, indicating the formation of compensatory-adaptive mechanisms and restoration of implant functional integrity. Follow-up SCTA demonstrated patency in the implantation zone without visible stenosis (Figure 15 a, b). Macroscopically, the matrix appearance was practically indistinguishable from the native vein. At explantation, signs of outer layer formation (neoadventitia) and graft surface neovascularization were noted. Matrix isolation from surrounding tissues was difficult due to integration, but no gross scarring, deformation, or aneurysmal changes were found (Figure 16).

***Figure 15:*** *SCTA follow-up of the biodegradable polymer matrix (BPM) implanted into the infrarenal segment of the posterior vena cava (animal No. 2):* **(a)** *follow-up at 12 months;* **(b)** *follow-up at 29 months. The implantation zone is patent, with no signs of stenosis.*

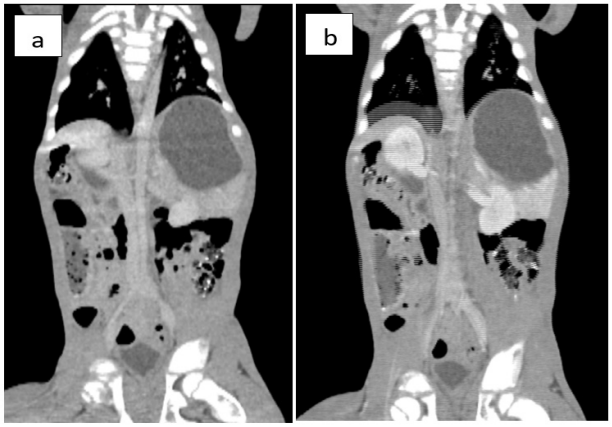


***Figure 16****: Macroscopic appearance of the implanted biodegradable polymer matrix (BPM) in animal No. 2.* **(a)** *Intraoperative image during primary implantation.* **(b)** *Appearance of the implant 29 months after implantation. Signs of outer layer formation (neoadventitia, arrow 1) and graft surface neovascularization (arrow 2) are noted. Isolation of the matrix from surrounding tissues was difficult due to integration; however, no gross scarring, deformation, or aneurysmal changes were detected.*

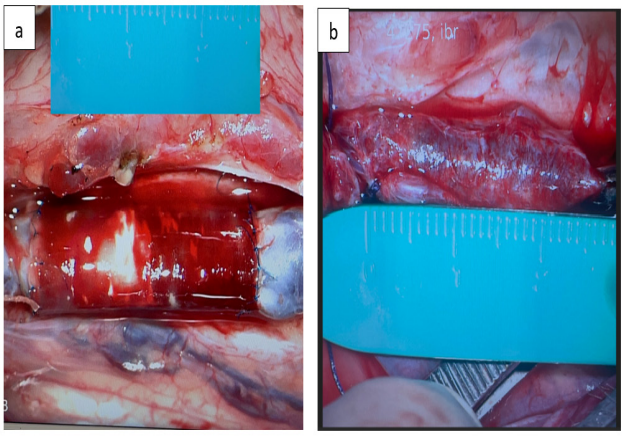


Histopathological examination revealed that the tissue-engineered vascular implant wall consisted of three clearly differentiated layers: neointima, neomedia, and neoadventitia. In the anastomotic zone with the posterior vena cava, no signs of myointimal hyperplasia were detected. A smooth transition of the native vessel intima onto the implant was observed (Figure 17). Thus, BPM demonstrated a balanced adaptive response, key characteristics of which include: pronounced and confirmed growth potential, reversibility of early constrictive changes, absence of intimal hyperplasia and degenerative changes, and stabilization of hemodynamic parameters in the long term. These data allow the observed constrictive phenomenon to be considered not as implant failure, but as a reversible stage of remodeling overcome during integration, supporting the promise of further optimization of this material class.

**PTFE prosthesis:** The polytetrafluoroethylene prosthesis showed no signs of adaptive remodeling. Its length and diameter remained unchanged (Figure 3 a, b). According to DUS and SCTA, the graft lost patency early due to thrombosis (Figure 18 b), confirmed intraoperatively at explantation (Figure 19 c). Histopathological examination verified luminal thrombosis with focal recanalization and calcification in the absence of true vascular wall formation (Figure 20), morphologically explaining its complete functional failure.

***Figure 17:*** *Fragment of the tissue-engineered vascular implant (BPM) wall 29 months after implantation. Hematoxylin and eosin staining, magnification ×10. Designations: EC - endothelial cells lining the inner surface; SMC - smooth muscle cells forming the medial layer; PLA - remnants of polymer fibers. Formation of a three-layer wall structure close to the native vein is observed.*

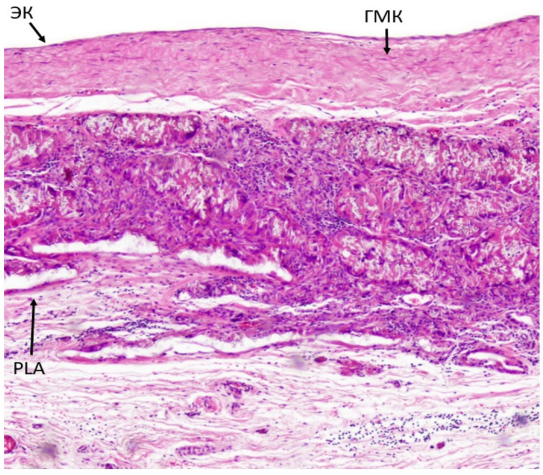


***Figure 18:*** *Ultrasound (***a***) and SCTA imaging (***b***) of the thrombosed PTFE prosthesis. Absence of blood flow in the prosthesis lumen (1), signs of occlusion. These findings correspond to the early loss of patency recorded during follow-up.*

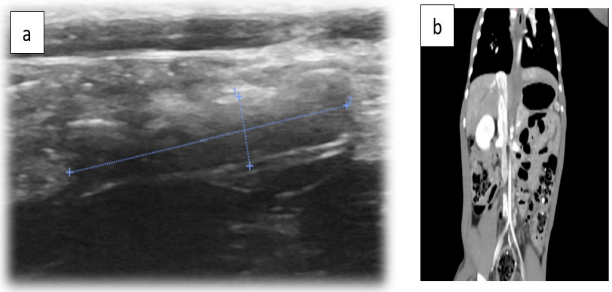


***Figure 19:*** *Macroscopic appeaance of the PTFE prosthesis in animal No. 1.* **(a)** *Intraoperative image during primary implantation.* **(b)** *Appearance of the prosthesis 29 months after implantation.* **(c)** *An organized thrombus is visualized in the graft lumen (indicated by the arrow).*

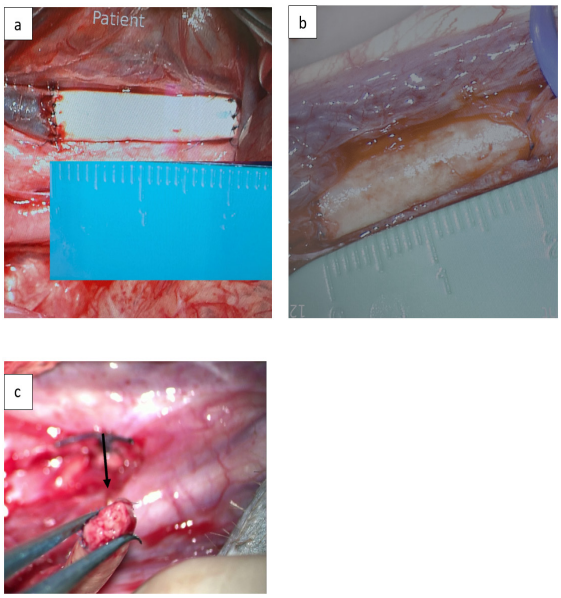

***Figure 20:*** *Cross-section of the PTFE prosthesis 29 months after implantation. Hematoxylin and eosin staining, magnification ×4. Designations: 1 - organized thrombus filling the lumen; 2 - recanalization zones within the thrombus; 3 (arrow) - prosthesis wall with signs of calcification. No true vascular wall formation is observed.*

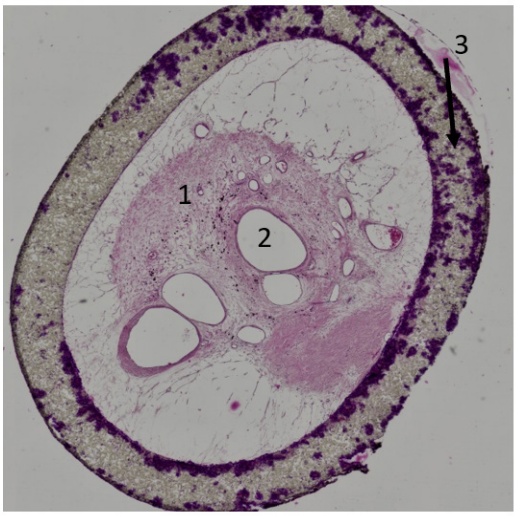


## Discussion

This pilot study in growing primates addressed a key problem in pediatric vascular surgery-the choice of optimal implant for major vein reconstruction under conditions of ongoing body growth. The developed experimental model proved adequate, as confirmed by significant increases in body length and weight in all animals during the 29-month observation period, modeling the phase of active somatic growth in children.

The central finding is the comprehensive evaluation of remodeling in different venous graft types using complementary methods-direct intraoperative morphometry and dynamic duplex ultrasound scanning (DUS). The autologous vein confirmed its "gold standard" status, demonstrating balanced physiological remodeling with proportional increases in length and diameter, complete integration into the vascular bed, and stable hemodynamics. However, autologous vein implantation is not always feasible in clinical pediatric practice, limiting surgical options.

Allogeneic grafts (both single-group and cross-group) exhibited significant but variable adaptive potential. They showed considerable length growth capacity (58–67% increase by morphometry), adequately responding to organism growth. However, the remodeling pattern of their diameter proved complex and method-dependent. The discrepancy observed in the single-group allograft between morphometry data (22% diameter decrease) and DUS (16% increasing trend) indicates the existence of compensatory hemodynamic mechanisms ensuring satisfactory function despite structural wall changes. Clinically, both allograft types performed as viable alternatives, justifying their use when autologous vein is unavailable. The biodegradable polymer matrix exhibited a phased remodeling pattern. The largest absolute length increase among all implants was recorded: +42% (19 to 27 mm), confirmed by both methods. Early postoperative constrictive remodeling was noted: anatomical diameter decreased by 33%, functional lumen by DUS narrowed by approximately 15%. However, by study end, a trend towards diameter restoration to near-baseline values was observed. Constriction was transient and reversible, not a progressive stenotic process.

Initial hemodynamic changes-increased linear velocity and decreased volumetric flow-normalized over time. By the end of observation, the pressure gradient stabilized, indicating restored implant functional integrity. Histological examination revealed no intimal hyperplasia. The polymer scaffold was replaced by connective tissue forming a three-layer structure close to native vein. Inflammatory reaction was minimal. Thus, the biodegradable matrix demonstrated a balanced adaptive response characterized by growth potential, reversibility of early constrictive changes, absence of intimal hyperplasia, and long-term hemodynamic stabilization. The observed constrictive phenomenon may be considered a reversible remodeling stage. These data suggest this material class is promising for further optimization.

An important methodological outcome is the demonstration of dissociation between structural changes and functional remodeling outcomes, as well as the high informativeness of combined morphometry and DUS.

**Study limitations:** This is a pilot study with a small sample size, due to the complexity and duration of primate experiments. The findings require verification in larger animal cohorts.

## Conclusion

- The developed model of posterior vena cava grafting in growing primates adequately reproduces conditions of ongoing growth and represents a relevant platform for preclinical evaluation of vascular implants for pediatric practice.
- A fundamental criterion for successful integration is established-the implant's ability to maintain stable hemodynamics, necessitating mandatory functional monitoring.
- The autologous vein retains "gold standard" status due to reproducible balanced remodeling and complete integration.
- Allogeneic grafts (single-group and cross-group) are a clinically viable alternative, possessing significant growth potential; their use requires dynamic ultrasound monitoring due to variable wall remodeling.
- The biodegradable polymer matrix exhibited a phased remodeling pattern: length increase (+42%) combined with reversible transient constrictive diameter change that resolved by study end. Absence of intimal hyperplasia and hemodynamic stabilization make this implant type promising for further optimization.
- The combination of direct morphometry, dynamic DUS monitoring, and histopathological verification represents an optimal methodological approach for comprehensive preclinical evaluation of vascular implants intended for growing organisms.

Thus, the study revealed that successful long-term implant remodeling under growth conditions is characterized not only by the ability to increase in size but primarily by balanced geometric changes, preservation of normal hemodynamics, and morphologically confirmed adequate transformation of wall structure. Only the autologous vein fully met these criteria. Allogeneic grafts showed clinically acceptable functional performance. The biodegradable matrix, possessing maximal growth potential, demonstrated reversibility of early constrictive changes and long-term functional stabilization in the absence of intimal hyperplasia, making it a promising material for further development. The obtained data confirm the high informativeness and complementarity of the comprehensive approach including morphometry, DUS, and histological analysis.

## Funding

Study design development, data analysis, and processing were supported by state funding for scientific activities at Academician I.P. Pavlov First St. Petersburg State Medical University (registration number 1025021900067-3).

## Conflict of Interest

The authors declare no conflict of interest.


## Acknowledgments

The research was carried out at the «Primat» Shared Research Facilities using its equipment.

The authors express their sincere gratitude to the staff of the Kurchatov Complex of Medical Primatology for their invaluable advisory support and for enabling the experimental part of the study: Stanislav A. Fokin, Head of the Complex; Mikhail S. Starchenkov, Head of the Surgical Department; Roman V. Panfilov, Veterinary Traumatologist; Daria S. Zhukova, Head of the Veterinary Department; Maria A. Anosova, Veterinary Anesthesiologist; Garina Zh. Kochkonyan, Head of the Nursery; and Larisa A. Burachek, Senior Zootechnician.


## References


1. Sadamori H, Hasegawa K, Oba A, Kato Y, Soejima Y, et al. (2024) Short- and long-term outcomes of liver resection with hepatic vein reconstruction for liver tumors: A nationwide multicenter survey. J Hepatobiliary Pancreat Sci 31(12):863-875.
2. Morse AK, Dobrila J, Salazar JD, LaPar DJ (2024) Complete Resection of Aorticopulmonary Paraganglioma with Reconstruction in a Pediatric Patient. Ann Thorac Surg Short Rep 2(3): 410-413.
3. Qureshi SS, MS, Dhareshwar J, Smriti V (2020) Limb sparing surgery with vascular reconstruction for nonrhabdomyosarcoma soft tissue sarcoma in infants: A novel solution using allogenic vein graft from the parent. J Pediatr Surg 55(8): 1673-1676.
4. Lejay A, Bratu B, Kuntz S, Neumann N, Heim F, Chakfé N (2023) Calcification of Synthetic Vascular Grafts: A Systematic Review. EJVES Vasc Forum. 60: 1-7.
5. Stetson A, Gutwein A, Bondoc A, Dasgupta R, Maijub J, et al. (2025) Interdisciplinary vascular reconstructive considerations for pediatric tumors. J Vasc Surg. S0741-5214(25)01875-0.
6. Shoji T, Shinoka T (2018) Tissue engineered vascular grafts for pediatric cardiac surgery. Transl Pediatr 7(2):188-195.
7. Cittadella G, de Mel A, Dee R, De Coppi P, Seifalian AM (2013) Arterial tissue regeneration for pediatric applications: inspiration from up-to-date tissue-engineered vascular bypass grafts. Artif Organs. 37(5): 423-434.
8. West-Livingston L, Lim JW, Lee SJ (2023) Translational tissue-engineered vascular grafts: From bench to bedside. Biomaterials. 302: 122322.
9. Piterina AV, Cloonan AJ, Meaney CL, Davis LM, Callanan A, et al. (2009) ECM-based materials in cardiovascular applications: Inherent healing potential and augmentation of native regenerative processes. Int J Mol Sci. 10(10): 4375-4417.
10. Anderson DEJ, Pohan G, Raman J, Konecny F, Yim EKF, et al. (2018) Improving Surgical Methods for Studying Vascular Grafts in Animal Models. Tissue Eng Part C Methods. 24(8):457-464.
11. Anderson DE, Glynn JJ, Song HK, Hinds MT (2014) Engineering an endothelialized vascular graft: a rational approach to study design in a non-human primate model. PLoS One. 9(12): e115163.
12. Keough EM, Callow AD, Connolly RJ, Weinberg KS, Aalberg JJ, et al. (1984) Healing pattern of small caliber dacron grafts in the baboon: an animal model for the study of vascular prostheses. J Biomed Mater Res 18(3):281-292.